Analytica Chimica Acta 1127 (2020) 156–162

Contents lists available at ScienceDirect

Analytica Chimica Acta

journal homepage: www.elsevier.com/locate/aca

Highly sensitive detection of carcinoembryonic antigen using copper-free click chemistry on the surface of azide cofunctionalized graphene oxide

Wenwen Xiang [1], Zhongjing Zhang [1], Wanqing Weng , Boda Wu , Jia Cheng , Liang Shi , Hongwei Sun , Li Gao [*], Keqing Shi [**]

Precision Medical Center Laboratory, The First Affiliated Hospital, Wenzhou Medical University, Wenzhou, 325015, China

HIGHLIGHTS

- A fluorescence biosensor based on carbon dots (CDs) was developed.
- Azide cofunctionalized graphene oxide quenched the fluorescence with copper-free click chemistry.
- The method has high sensitivity and good selectivity.

GRAPHICAL ABSTRACT

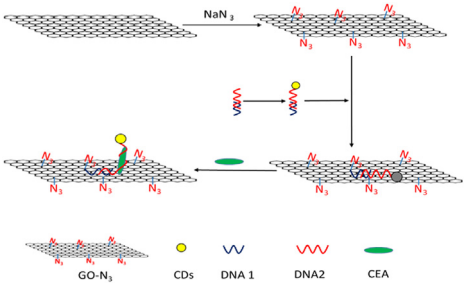

ARTICLE INFO

Article history:
Received 28 May 2020
Received in revised form
19 June 2020
Accepted 22 June 2020
Available online 10 July 2020

Keywords:
Carcinoembryonic antigens
Biosensor
Copper-free click chemistry
Carbon dots
Azide cofunctionalized graphene oxide

ABSTRACT

In this study, we reported a highly sensitive method for detecting carcinoembryonic antigen (CEA) based on an azide cofunctionalized graphene oxide (GO-N_3) and carbon dot (CDs) biosensor system. Carbon dots-labeled DNA (CDs-DNA) combined with GO-N_3 using copper-free click chemistry (CFCC), which quenched the fluorescence of the CDs via fluorescence resonance energy transfer (FRET). Upon the addition of CEA, fluorescence was recovered due to the combination of CEA and aptamer. Under optimal conditions, the relative fluorescence intensity was linear with CEA concentration in the range of 0.01 −1 ng/mL ($R^2 = 0.9788$), and the limit of detection (LOD) was 7.32 pg/mL (S/N = 3). This biosensor had a high sensitivity and good selectivity for CEA detection in serum samples, indicating that the novel sensor platform holds a great potential for CEA and other biomarkers in practical applications.

1. Introduction

Cancer, also known as malignant tumor, is one of the diseases that seriously threaten human health and life. Carcinoembryonic antigen (CEA) is an acidic glycoprotein, also a tumor marker, which has important clinical value in the differential diagnosis, condition monitoring and therapeutic evaluation of diseases [1–3]. CEA expression is largely inhibited after birth which has only low levels in the plasma of healthy adults [4]. The concentration of CEA about 5 μg/L in healthy people, and the concentration exceeding 20 μg/L is considered an indicator of cancer [5,6]. It is overexpressed in many

* Corresponding author.
** Corresponding author.
E-mail address: guobeijing@pku.edu.cn (L. Gao).
[1] These authors contributed equally.

https://doi.org/10.1016/j.aca.2020.06.053
0003-2670/

human cancers, such as gastric cancer, colorectal cancer, breast cancer, ovarian cancer, lung cancer, and pancreatic cancer [7–9]. Currently, more and more methods were being used to detect CEA in actual samples with the development of analytical techniques. Traditional detection methods are mainly based on immunoassay techniques, including enzyme-linked immunosorbent assays (ELISAs) [10],radioimmunoassay [11], surface enhanced raman scattering immunoassay [12] and electrochemical immunoassay [13] etc.. Compared with antibodies, aptamers have many advantages, such as fast response, low cost, easy access to chemical synthesis, high accuracy, good repeatability, flexible labeling and good stability [14,15]. Therefore, aptamer biosensors have attracted great attention as a tool for fast, simple, and low-cost analysis and diagnostic applications.

When the spectrum of the donor fluorescent molecule overlapped with the excitation spectrum of the acceptor molecule, excitation of the donor fluorescent molecule induced fluorescence of the acceptor molecule while the fluorescence intensity of the donor fluorescent molecule was diminished. This phenomenon is called fluorescence resonance energy transfer (FRET) [16,17]. FRET-based sensors are sensitive, fast, simple, low cost, and have been widely used for protein detection [18–20].

Compared to organic fluorophores, quantum dots (QDs) have unique optical properties, including good chemical stability, broad absorption and narrow emission wavelength, and easy functionalization, which made it widely used in fluorescence probe and medical imaging [21,22]. However, the use of QDs have certain limitations due to its potential toxicity and high background signals for detecting biomolecules [23]. The newly emerging carbon dots (CDs) solved these problems very well [24]. Carbon dots (CDs) are spherical carbon-based fluorescent nanoparticles, typically < 10 nm in diameter [25]. Since its discovery in 2004, the CDs have challenged the concept that carbon materials are black and dark, drawing widespread attention from researchers [26,27]. Recently, CDs have become a superior and versatile fluorophore, which is widely used in fluorescence sensors due to its ease synthesis, low toxicity and small size. In addition, CDs also have the advantages of excellent water dispersibility, excellent chemical and colloidal stability, good biocompatibility, and easy surface modification [24,28–30].

Studies in the last several decades have shown that click reaction has proved to be a very simple and efficient method for signal translation, surface modification and bio-conjugation of nanomaterials [31–33]. The concept of "click chemistry" was first proposed by Sharpless et al in 2001 [31]. It is typically a Cu-catalyzed bio-orthogonal reaction between alkyne and azide groups [34]. This type of organic reaction is selective, simplicity, moderate reaction conditions, and does not produce high efficiency by-products in aqueous solvents at room temperature [35–37]. However, Cu(I) has certain toxicity as a catalyst [38] and Cu(I) catalyst used in the click chemistry can efficiently and irreversibly quench the QDs fluorescence [39]. Some examples of in vitro copper-induced degradation of viruses or oligonucleotide strands have been reported [40]. The copper-free click chemistry (CFCC) was first developed by Bertozzi et al. [41]. It removes the adverse effects of copper ions and simplifies the experimental procedure, becoming a promising alternative to copper(I)-catalyzed alkyne-azide cycloaddition (CuAAC).

Here, we reported a fluorescence biosensor based on CDs and click reaction for detecting the CEA. DNA1 modified with dibenzyl cyclooctyne (DBCO) hybridized to DNA2 modified with amino to form DNA3. CDs-DNA was immobilized on the surface of graphene oxide by click chemistry between azide-functionalized graphene oxide (GO-N_3) and DNA with DBCO group. The fluorescence of CDs was quenched by GO. After CEA was added, the combination of CEA and aptamer induced a change in the conformation of aptamer, and the departure of CD from the surface of GO resulted in fluorescence recovery (see Fig. 1). Compared with physical adsorption, this method can solve the problems of non-specific probe displacement and false positive signals.

2. Experimental

2.1. Chemicals and materials

DNA1: 5' -TCT CTC TCT CTC TTT TTT TTT-3′-NH_2; DNA2 (containing aptamer sequence): 5' -GAG AGA GAG AGA ATA CCA GCT TAT TCA ATT -3′-DBCO. All DNA sequence were synthesized by Sangon Biotech (Shanghai) Co., Ltd. and purified by HPLC and mass spectrometry. CEA was acquired from Shanghai Linc-Bio Co., Ltd. BSA, IgG, thrombin, uric acid, N-hydroxysuccinimide (NHS) and 1-ethyl-3-(3-dimethylaminopropyl)-carbodiimide (EDC) were provided from Sigma-Aldrich. Glucose, sodium azide (NaN_3), N, N-dimethylformamide (DMF), citric acid, ethylenediamine, NaOH, sodium chloroacetate ($ClCHClCH_2COONa_2$) and HCl were purchased from Sinopharm Chemical Reagent Co., Ltd. VEGF, Tube-O-DIALYZER was obtained from Sangon Biotech (Shanghai) Co., Ltd. Serum was supplied by Zhejiang Tianhang Biotechnology Co., Ltd. PBS was purchased from Shanghai Double-helix biotech Co., Ltd. The solution used in the experiment was prepared with ultrapure water (18.25 MΩ cm).

2.2. Apparatus

All fluorescence measurements were performed on a Bio-Tek Synergy H4 multi-function microplate reader, and fluorescence spectra were collected at 380 nm excitation. FT-IR spectra were obtained in transmission mode using the American Thermoelectric Nicolet iS50. TEM images were obtained at 200 KV using High Resolution Transmission Electron Microscope (JEM-2100 (HR)). The sample was freeze-dried using a vacuum freeze dryer (FD-1A-50). Ultrapure water was prepared by Sichuan Yupu ultrapure water machine (18.25 MΩ cm). The pH of the solution was measured using PHS-25 digital viscometer.

2.3. Preparation of CDs-DNA

CDs were prepared according to the previously reported method [42,43]. Briefly, Citric acid (3.0 g) and ethylenediamine (1875 μL) were dissolved in ultrapure water (30 mL). Then solution was transferred to a Teflon-lined autoclave (50 mL) and heated at 180 °C for 8 h. Product was taken out after cooling to room temperature. Then it was dialyzed against ultrapure water for 48 h (Molecular Weight Cutoff, 4 KDa), and lyophilized 16 h to obtain CDs. 10 mg of CDs were dispersed in ultrapure water (10 mL) containing 0.5 g of NaOH and 0.5 g of sodium chloroacetate, followed by sonication for 2 h. The product was neutralized with acid and dialyzed against ultrapure water for 48 h to obtain CDs-COOH (Molecular Weight Cutoff: 4 KDa), which was lyophilized 16 h for use [44]. At the same concentration, an equal volume of DNA1 and DNA2 were mixed, placed in a water bath at 95 °C for 5 min, and taken out at room temperature for 2 h to obtain DNA 3 (5 μM).

The prepared CDs-COOH was dissolved in ultrapure water to prepare a solution of 10 mg/mL CDs-COOH. A solution of 250 mM NHS (1 mL) and 2.5 M EDC (1 mL) was added to a 10 mg/mL solution of CDs-COOH (1 mL), and then the mixture was sonicated for 2 h. DNA 3 (5 μM) and prepared CDs-COOH were mixed in an equal volume, and reacted at 4 °C overnight to obtain CDs-DNA. The product was dialyzed for 24 h to remove excess CDs-COOH (Molecular Weight Cutoff, 15 KDa). The concentration of CDs-DNA was

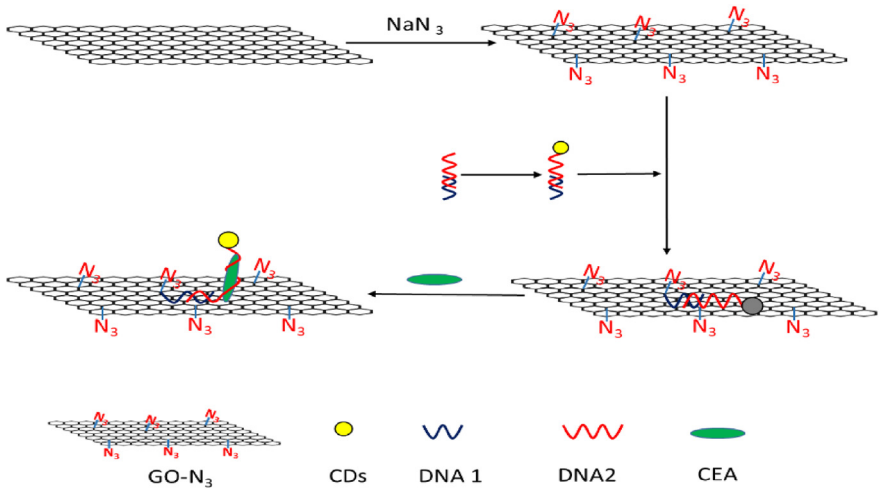

Fig. 1. Schematic illustration of CEA detection system based on click chemistry and FRET between GO-N_3 and CDs-DNA.

quantified based on UV–vis absorption at a concentration of CDs-COOH at 335 nm [42].

2.4. Preparation of GO-N_3

Graphene oxide (GO) was prepared from graphite powder by the classical Hummers method [45] and GO-N_3 was prepared according to the previously reported method [46]. GO (0.1 g) and DMF (200 mL) were sonicated for 3 h, then NaN_3 (1 g) and reacted at 40 °C for 48 h. Unreacted NaN_3 was removed by washing with DMF, followed by centrifugation three times at 12, 000 rpm for 25 min, and the product was lyophilized to obtain GO-N_3. Dried GO-N_3 was added to 5 mL of ultrapure water to prepare an aqueous solution, ultrasound 2 h (2 mg/mL).

2.5. Detection of CEA

CDs-DNA (25 μg/mL) and GO-N_3 (10 μg/mL) were added to 600 μL of PBS (10 mM, pH = 7.5), and reacted at 25 °C for 3 h. Unbound CDs-DNA was removed using the centrifugation (15, 000 rpm, 30 min). Then, different concentrations of CEA were added to the reaction solution, and incubated at 25 °C for half an hour. We measured the fluorescence spectrum at 380 nm excitation. The value of signal (F/F_0 -1) was calculated from the fluorescence intensity at 450 nm, where F_0 and F represented the fluorescence intensity of the GO-N_3 based biosensor system before or after the addition of CEA. Each set of data was measured in triplicate and the average fluorescence signal was obtained.

3. Results and discussion

3.1. Characterization of GO-N_3

Fig. 2A and B and C were TEM images of GO-N_3, CDs and GO-N_3-CDs-DNA. The typical GO morphology, and inherent wrinkles and folds of GO could be observed (Fig. 2A). Fig. 2B and 2C showed the spherical structure of the CDs and the CDs were uniformly linked on the surface of the GO-N_3. The size of the carbon dots was uniform from the TEM image (Fig. 2B), about 5 nm. Additionally, the emission spectra of CDs with the excitations from 360 to 420 nm were recorded (Fig. 2D). When the excitation wavelength was 380 nm, the maximum fluorescence emission wavelength of CDs was 450 nm. This was consistent with the previously reported method [43]. Fig. 2E was the FTIR spectra of GO, GO-N_3 and GO-N_3-CDs-DNA. Several characteristic peaks of GO were observed in the FT-IR spectrum including the peaks at 3386, 1718, 1618 and 1050 cm^{-1}, due to O–H stretching vibration, C=O stretching vibration, C–OH stretching vibration, and C–O stretching vibration, respectively [47–49]. The peak observed at 2124 cm^{-1} could be attributed to the absorption of the azide group, indicating that we successfully synthesized GO-N_3 [46,50]. The peaks of 2934, 1575 and 1235 cm^{-1} for GO-N_3-CDs-DNA were characteristic of C–H, -N-C=O and NHC=O stretching vibration respectively. These results showed that CDs-DNA was successfully linked to GO-N_3 [42,51].

3.2. Optimization of assaying conditions

In order to achieve optimal detection conditions, we optimized the experimental conditions, including GO-N_3 concentration, CDs-DNA concentration, pH, incubation temperature, and reaction time for detecting CEA. First, we studied the effect of GO-N_3 concentration on the sensor. We chose different concentrations of GO-N_3 (4, 6, 8, 10, 12 and 15 μg/mL) to quench the fluorescence of CDs. The same concentration of CEA was added to the sensor to measure the fluorescence intensity, and the value of F/F_0-1 was compared. The results showed that the value of F/F_0 -1 also increased with the concentration of GO-N_3 increasing and reaching a maximum at 10 μg/mL (Fig. 3A). And F/F_0-1 would decrease with the concentration higher than 10 μg/mL. Low concentrations of GO-N_3 were not conducive for CDs-DNA immobilization. The excessive concentrations of GO-N_3 resulted in lower fluorescence intensity and were not conducive to the recovery of fluorescence. Therefore, 10 μg/mL was used in the subsequent experiments. In the same way, the concentrations of CDs-DNA were optimized and found that the value of F/F_0-1 was best at 25 μg/mL (Fig. 3B). Low concentrations of CDs-DNA were not conducive to the recovery of fluorescence, and excessive concentrations leaded to an increase in background signal, which in turn led to a decrease in the growth rate. The different pH values (5, 6, 7, 7.5, 8 and 9) were evaluated to the sensors and the value of F/F_0-1 was best at pH 7.5 (Fig. 3C). The different incubation temperatures (4 °C, 25 °C, 37 °C, 50 °C and 70 °C) were explored. 25 °C was selected based on the results (Fig. 3D). Finally, the incubation time was studied and 30 min was selected for the sensors (Fig. 3E).

3.3. Sensitivity for assaying CEA

Different concentrations of CEA were added into the sensor

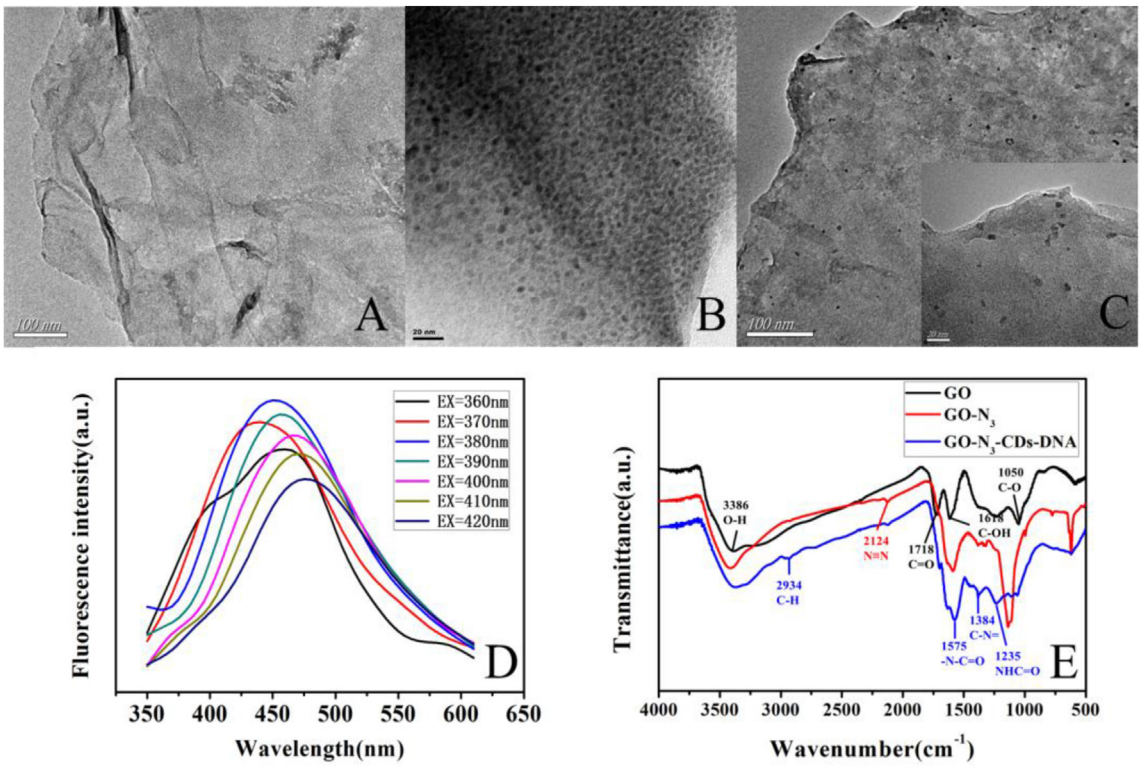

Fig. 2. A) TEM image of GO-N_3. B) TEM image of CDs. C) TEM image of GO-N_3-CDs-DNA. D) Fluorescence emission spectra of CDs for varying excitation wavelengths. E) FT-IR spectrums of GO, GO-N_3 and GO-N_3-CDs-DNA.

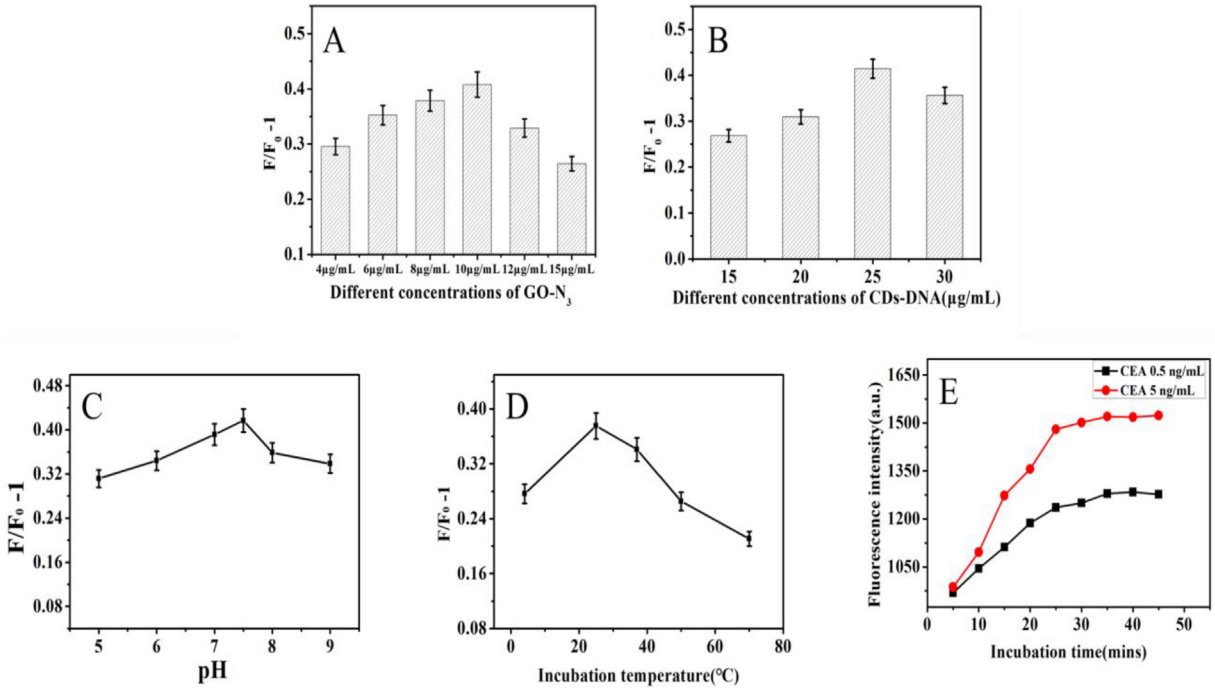

Fig. 3. Effects of A) different concentrations of GO-N_3, B) different concentrations of CDs-DNA, C) different pH values, D) different temperatures and E) different incubation times for the sensors. The CEA concentration was 0.8 ng/mL.

containing GO-N_3 and CDs-DNA in PBS buffer solution. The conformation of the aptamer would be changed after CEA bound to the aptamer, which resulted in the recovery of fluorescence. Under optimal conditions, different concentrations of CEA (0–50 ng/mL) were added into the sensors and incubated for 30 min at 25 °C. The fluorescence spectrum at excitation of 380 nm was measured and F/

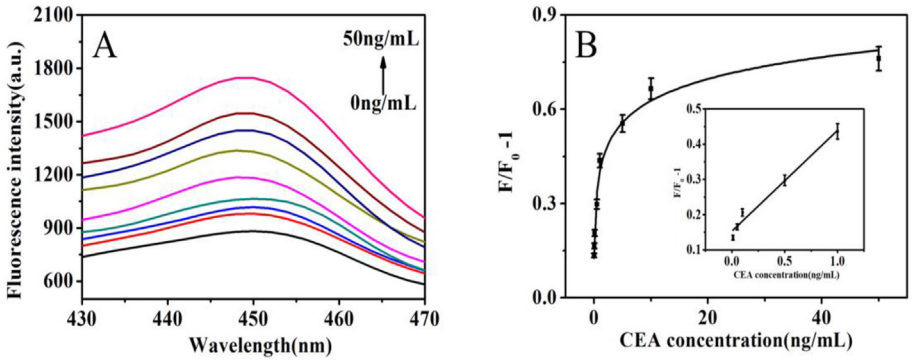

Fig. 4. A) Fluorescence spectra of GO-N_3 and CDs-DNA based sensor systems containing various concentrations of CEA (0, 0.01, 0.05, 0.1, 0.5, 1, 5, 10 and 50 ng/mL); B) Relationship between different concentrations of CEA and F/F_0 -1 (450 nm).

F_0 -1 at 450 nm was calculated. The results were shown in Fig. 4A. The fluorescence recovery depended on the concentration of CEA, and the fluorescence intensity increased with the increase of CEA concentrations. The fluorescence growth was relatively slow with the concentrations of CEA increasing. The value of F/F_0-1 were linear with low concentrations of CEA between 0.01 and 1 ng/mL (Fig. 4 B). The linear regression equation was $F/F_0 - 1 = 0.287 \times C_{[CEA]} + 0.153$ (C referred to the concentration), $R^2 = 0.979$. The detection limit (LOD) was calculated to be 7.32 pg/mL based on 3 S/N. Compared with other CEA aptamer sensors, the sensor in this study had a lower detection limit and a good linear range, which was better than other sensors. The detection limit of CEA observed in this study was comparatively better than that obtained from other assays (as shown in Table 1).

3.4. Selectivity for assaying CEA

Selectivity is an important parameter for evaluating the performance of sensors. Several different substances (CEA, BSA, IgG, VEGF, thrombin, uric acid and glucose) were selected to evaluate the selectivity of the sensor. 5 ng/mL CEA and other interferences with the concentration of 50 ng/mL (BSA, IgG, VEGF, thrombin, uric acid and glucose) were added to the sensor. Even if the interference concentration was 10 times the concentration of CEA, it did not cause a significant increase in the fluorescence intensity (Fig. 5). The change of fluorescence intensity caused by CEA could still be distinguished from other substances. The result showed that the sensor had a good selectivity.

3.5. Analysis of CEA in serum

To verify the practical application of the sensor, three concentrations (0.1, 0.5, and 1 ng/mL) of CEA were selected for the standard recovery experiments in serum. Each experiment was repeated three times and the results were shown in Table 2. The

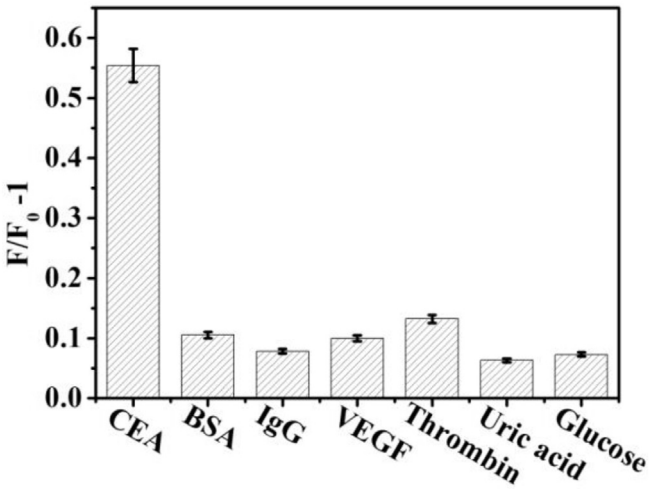

Fig. 5. Selectivity of CEA (5 ng/mL) with other interfering substances such as BSA, IgG, VEGF, thrombin, uric acid, and glucose (50 ng/mL).

Table 2
Results for the determination of CEA in the serum (n = 3).

Samples	Added (ng/mL)	obtained (ng/mL)	Recovery (%)	RSD (%)
1	0.1	0.10291	102.91	3.38
2	0.5	0.51786	103.572	4.46
3	1	0.99265	99.265	1.11

Table 1
A comparison of our method with other methods for CEA detection.

Method	Assay strategy	Linear range	LOD	Ref
Colorimetric	Salt-induced AuNPs aggregation	0–120 ng/mL	3 ng/mL	[52]
Colorimetric	Label-free optical strategy	1–50 ng/mL	1 ng/mL	[53]
Fluorescence	Synthesize the blue-fluorescent carbon dots with tomato juice	1 ng/mL to 0.5 mg/mL	0.3 ng/mL	[54]
Fluorescence	“Mix-and-detect” procedure	0.4–100 ng/mL	0.316 ng/mL	[55]
Fluorescence	Polymer point based FRET	0.1–10 ng/mL	–	[20]
Fluorescence	FRET between upconversion nanoparticles (UCNPs) and graphene oxide (GO)	0.03–6 ng/mL	7.9 pg/mL	[56]
Fluorescence	Handing system based on embedded technology	1–100 ng/mL	0.049 ng/mL	[57]
Chemiluminescence (CL)	All-in-one dual-aptasensor	0–200 ng/mL	0.58 ng/mL	[58]
Electrochemiluminescence (ECL)	Label-free ECL	0.05–20 ng/mL	0.031 ng/mL	[59]
Electrochemistry	Sandwich complexes	1–200 ng/mL	0.5 ng/mL	[60]
Electrochemistry	Dual-analyte detection system	1 ng/mL to 1 μg/mL	0.517 ng/mL	[61]
Fluorescence	Carbon Dots-Labeled aptasensor	0.01–1 ng/mL	7.32 pg/mL	This work

recovery rate was from 99.27% to 103.57% and the relative standard deviation (RSD) was controlled at 1.11%–4.46%. It showed that the sensor had an analytical significance in actual detection.

4. Conclusion

In this work, a sensor based on CDs and click reaction for highly sensitive detection of CEA was developed. This sensor rapidly induced the conjugation between GO-N_3 and CDs by click chemistry can solve the problem of non-specific probe displacement and false positive signals in the physical adsorption. The sensor was highly sensitive and highly selective to CEA. LOD was as low as 7.32 pg/mL and exhibited a good linear relationship in the range of 0.01–1 ng/mL. Three concentrations were selected to be carried out the experiments in serum, and the results showed this sensor is promising in the analysis of CEA.

CRediT authorship contribution statement

Wenwen Xiang: Formal analysis, Investigation, Methodology. **Zhongjing Zhang:** Formal analysis, Investigation, Methodology. **Wanqing Weng:** Data curation. **Boda Wu:** Data curation. **Jia Cheng:** Writing - original draft. **Liang Shi:** Writing - original draft. **Hongwei Sun:** Writing - original draft. **Li Gao:** Project administration, Supervision. **Keqing Shi:** Supervision, Writing - review & editing.

Declaration of competing interest

The authors declare that they have no known competing interests or personal relationships that could have appeared to influence the work reported in this paper.

Acknowledgements

This work is supported by the First Affiliated Hospital, Wenzhou Medical University (No.2018-770).

References

[1] Z. Liu, S. Lei, L. Zou, G. Li, L. Xu, B. Ye, A label-free and double recognition-amplification novel strategy for sensitive and accurate carcinoembryonic antigen assay, Biosens. Bioelectron. 131 (2019) 113–118.
[2] J.Y. Huang, L. Zhao, W. Lei, W. Wen, Y.J. Wang, T. Bao, H.Y. Xiong, X.H. Zhang, S.F. Wang, A high-sensitivity electrochemical aptasensor of carcinoembryonic antigen based on graphene quantum dots-ionic liquid-nafion nanomatrix and DNAzyme-assisted signal amplification strategy, Biosens. Bioelectron. 99 (2018) 28–33.
[3] G. Saito, S. Sadahiro, K. Okada, A. Tanaka, T. Suzuki, A. Kamijo, Relation between carcinoembryonic antigen levels in colon cancer tissue and serum carcinoembryonic antigen levels at initial surgery and recurrence, Oncology 91 (2016) 85–89.
[4] J.A. Hensel, V. Khattar, R. Ashton, S. Ponnazhagan, Recombinant AAV-CEA tumor vaccine in combination with an immune adjuvant breaks tolerance and provides protective immunity, Molecular Therapy Oncolytics 12 (2019) 41–48.
[5] M. Mazloum-Ardakani, Z. Tavakolian-Ardakani, N. Sahraei, S.M. Moshtaghioun, Fabrication of an ultrasensitive and selective electrochemical aptasensor to detect carcinoembryonic antigen by using a new nanocomposite, Biosens. Bioelectron. 129 (2019) 1–6.
[6] X. Gu, Z. She, T. Ma, S. Tian, H.B. Kraatz, Electrochemical detection of carcinoembryonic antigen, Biosens. Bioelectron. 102 (2018) 610–616.
[7] J. Han, Y. Li, J. Feng, M. Li, P. Wang, Z. Chen, Y. Dong, A novel sandwich-type immunosensor for detection of carcino-embryonic antigen using silver hybrid multiwalled carbon nanotubes/manganese dioxide, J. Electroanal. Chem. 786 (2017) 112–119.
[8] M.H. Tan, H.Y. Wang, C.H. Hsieh, C.N. Wen, Y.H. Wen, C.H. Chen, J.J. Lu, Cancers screening in an asymptomatic population by using multiple tumour markers, PloS One 11 (2016).
[9] S. Kumar, M. Umar, A. Saifi, S. Kumar, S. Augustine, S. Srivastava, B.D. Malhotra, Electrochemical paper based cancer biosensor using iron oxide nanoparticles decorated PEDOT: PSS, Anal. Chim. Acta 1056 (2019) 135–145.
[10] X. Wang, J. Hu, G. Zhang, S. Liu, Highly selective fluorogenic multianalyte biosensors constructed via enzyme-catalyzed coupling and aggregation-induced emission, J. Am. Chem. Soc. 136 (2014) 9890–9893.
[11] M. Cioffi, M.T. Vietri, P. Gazzerro, R. Magnetta, A. D'Auria, A. Durante, E. Nola, G.A. Puca, A.M. Molinari, Serum anti-p53 antibodies in lung cancer: comparison with established tumor markers, Lung Canc. 33 (2001) 163–169.
[12] C. Hyangah, L. Sangyeop, S.S. Wook, O. Chil Hwan, C. Jaebum, Highly sensitive immunoassay of lung cancer marker carcinoembryonic antigen using surface-enhanced Raman scattering of hollow gold nanospheres, Anal. Chem. 81 (2009) 3029–3034.
[13] J. Huang, J. Tian, Y. Zhao, S. Zhao, Ag/Au nanoparticles coated graphene electrochemical sensor for ultrasensitive analysis of carcinoembryonic antigen in clinical immunoassay, Sensor. Actuator. B Chem. 206 (2015) 570–576.
[14] K. Hoon Young, B.J.B. Jonghoe, Therapeutics, nucleic acid aptamers: new methods for selection, stabilization, and application in biomedical science, Biomol.Therapeut. 21 (2013) 423–434.
[15] M. Yousefi, S. Dehghani, R. Nosrati, H. Zare, M. Evazalipour, J. Mosafer, B.S. Tehrani, A. Pasdar, A. Mokhtarzadeh, M. Ramezani, Aptasensors as a new sensing technology developed for the detection of MUC1 mucin: a review, Biosens. Bioelectron. 130 (2019) 1–19.
[16] N. Xia, F. Feng, C. Liu, R. Li, W. Xiang, H. Shi, L. Gao, The detection of mercury ion using DNA as sensors based on fluorescence resonance energy transfer, Talanta 192 (2019) 500–507.
[17] V.T. Forster, Zwischenmolekulare energiewanderung und fluoreszenz, Ann Phys-Berlin 437 (1948) 55–75.
[18] S.E. Wang, S. Si, A fluorescent nanoprobe based on graphene oxide fluorescence resonance energy transfer for the rapid determination of oncoprotein vascular endothelial growth factor (VEGF), Appl. Spectrosc. 67 (2013) 1270–1274.
[19] X. Wang, A. Jiang, T. Hou, H. Li, F. Li, Enzyme-free and label-free fluorescence aptasensing strategy for highly sensitive detection of protein based on target-triggered hybridization chain reaction amplification, Biosens. Bioelectron. 70 (2015) 324–329.
[20] Z. Lin, G. Zhang, W. Yang, B. Qiu, G. Chen, CEA fluorescence biosensor based on the FRET between polymer dots and Au nanoparticles, Chem. Commun. 48 (2012) 9918–9920.
[21] Z. Qiu, J. Shu, D. Tang, Bioresponsive release system for visual fluorescence detection of carcinoembryonic antigen from mesoporous silica nanocontainers mediated optical color on quantum dot-enzyme-impregnated paper, Anal. Chem. 89 (2017) 5152–5160.
[22] Z.M. Zhou, J. Zhou, J. Chen, R.N. Yu, M.Z. Zhang, J.T. Song, Y.D. Zhao, Carcinoembryonic antigen detection based on fluorescence resonance energy transfer between quantum dots and graphene oxide, Biosens. Bioelectron. 59 (2014) 397–403.
[23] S. Hamd-Ghadareh, A. Salimi, F. Fathi, S. Bahrami, An amplified comparative fluorescence resonance energy transfer immunosensing of CA125 tumor marker and ovarian cancer cells using green and economic carbon dots for bio-applications in labeling, imaging and sensing, Biosens. Bioelectron. 96 (2017) 308–316.
[24] P. Devi, S. Saini, K.H. Kim, The advanced role of carbon quantum dots in nanomedical applications, Biosens. Bioelectron. 141 (2019) 111158.
[25] C. Gu, C. Guo, Z. Li, M. Wang, N. Zhou, L. He, Z. Zhang, M. Du, Bimetallic ZrHf-based metal-organic framework embedded with carbon dots: ultra-sensitive platform for early diagnosis of HER2 and HER2-overexpressed living cancer cells, Biosens. Bioelectron. 134 (2019) 8–15.
[26] X. Xu, R. Ray, Y. Gu, H.J. Ploehn, L. Gearheart, K. Raker, W.A. Scrivens, Electrophoretic analysis and purification of fluorescent single-walled carbon nanotube fragments, J. Am. Chem. Soc. 126 (2004) 12736–12737.
[27] B. Rezaei, H.R. Jamei, A.A. Ensafi, Lysozyme aptasensor based on a glassy carbon electrode modified with a nanocomposite consisting of multi-walled carbon nanotubes, poly (diallyl dimethyl ammonium chloride) and carbon quantum dots, Mikrochim. Acta 185 (2018) 180.
[28] D. Zhong, K. Yang, Y. Wang, X. Yang, Dual-channel sensing strategy based on gold nanoparticles cooperating with carbon dots and hairpin structure for assaying RNA and DNA, Talanta 175 (2017) 217–223.
[29] B. Wang, Y. Chen, Y. Wu, B. Weng, Y. Liu, Z. Lu, C.M. Li, C. Yu, Aptamer induced assembly of fluorescent nitrogen-doped carbon dots on gold nanoparticles for sensitive detection of AFB 1, Biosens. Bioelectron. 78 (2016) 23–30.
[30] X.T. Zheng, A. Ananthanarayanan, K.Q. Luo, P. Chen, Glowing graphene quantum dots and carbon dots: properties, syntheses, and biological applications, Small 11 (2015) 1620–1636.
[31] H.C. Kolb, M.G. Finn, K.B. Sharpless, Click chemistry: diverse chemical function from a few good reactions, Angew. Chem. Int. Ed. 40 (2001) 2004–2021.
[32] D. Toulemon, B.P. Pichon, C. Leuvrey, S. Zafeiratos, V. Papaefthimiou, X. Cattoën, S. Bégin-Colin, Fast assembling of magnetic iron oxide nanoparticles by microwave-assisted copper(I) catalyzed alkyne–azide cycloaddition (CuAAC), Chem. Mater. 25 (2013) 2849–2854.
[33] T. Ouyang, X. Liu, H. Ouyang, L. Ren, Recent trends in click chemistry as a promising technology for virus-related research, Virus Res. 256 (2018) 21–28.
[34] W. Zheng, H. Li, W. Chen, J. Zhang, N. Wang, X. Guo, X. Jiang, Rapid detection of copper in biological systems using click chemistry, Small 14 (2018), e1703857.
[35] Y. Chen, Y. Xianyu, J. Wu, B. Yin, X. Jiang, Click chemistry-mediated nanosensors for biochemical assays, Theranostics 6 (2016) 969–985.
[36] M.J. Banuls, M.A. Gonzalez-Martinez, J. Sabek, J. Garcia-Ruperez, A. Maquieira, Thiol-click photochemistry for surface functionalization applied to optical biosensing, Anal. Chim. Acta 1060 (2019) 103–113.

[37] J.F. Lutz, 1, 3-Dipolare Cycloaddition von Aziden und Alkinen: eine universelle Ligationsmethode in den Polymer- und Materialwissenschaften, Angew. Chem. Int. Ed. 119 (2007) 1036–1043.
[38] J.M. Baskin, J.A. Prescher, S.T. Laughlin, N.J. Agard, P.V. Chang, I.A. Miller, A. Lo, J.A. Codelli, C.R. Bertozzi, Copper-free click chemistry for dynamic in vivo imaging, Proc. Natl. Acad. Sci. U.S.A. 104 (2007) 16793–16797.
[39] H.Y. Zhang, G.Q. Feng, Y. Guo, D.J. Zhou, Robust and specific ratiometric biosensing using a copper-free clicked quantum dot-DNA aptamer sensor, Nanoscale 5 (2013) 10307–10315.
[40] J.F. Lutz, Copper-free azide-alkyne cycloadditions: new insights and perspectives, Angew. Chem. Int. Ed. 47 (2008) 2182–2184.
[41] N.J. Agard, J.A. Prescher, C.R. Bertozzi, A strain-promoted [3 + 2] azide–alkyne cycloaddition for covalent modification of biomolecules in living systems, J. Am. Chem. Soc. 126 (2004) 15046–15047.
[42] X. Cui, L. Zhu, J. Wu, Y. Hou, P. Wang, Z. Wang, M. Yang, A fluorescent biosensor based on carbon dots-labeled oligodeoxyribonucleotide and graphene oxide for mercury (II) detection, Biosens. Bioelectron. 63 (2015) 506–512.
[43] J. Zhu, X. Bai, J. Bai, G. Pan, Y. Zhu, Y. Zhai, H. Shao, X. Chen, B. Dong, H. Zhang, H. Song, Emitting color tunable carbon dots by adjusting solvent towards light-emitting devices, Nanotechnology 29 (2018), 085705.
[44] X. Sun, Z. Liu, K. Welsher, J.T. Robinson, A. Goodwin, S. Zaric, H. Dai, Nano-graphene oxide for cellular imaging and drug delivery, Nano Research 1 (2008) 203–212.
[45] W.S. Hummers, R.E. Offeman, Preparation of graphitic oxide, J. Am. Chem. Soc. 80 (1958), 1339-1339.
[46] T. Wei, T. Dong, H. Xing, Y. Liu, Z. Dai, Cucurbituril and azide cofunctionalized graphene oxide for ultrasensitive electro-click biosensing, Anal. Chem. 89 (2017) 12237–12243.
[47] Y. He, X. Xing, H. Tang, D. Pang, Graphene oxide-based fluorescent biosensor for protein detection via terminal protection of small-molecule-linked DNA, Small 9 (2013) 2097–2101.
[48] Y. Sun, J. Li, Y. Wang, C. Ding, Y. Lin, W. Sun, C. Luo, A chemiluminescence biosensor based on the adsorption recognition function between Fe_3O_4@SiO_2@GO polymers and DNA for ultrasensitive detection of DNA, Spectrochim. Acta Mol. Biomol. Spectrosc. 178 (2017) 1–7.
[49] A. Taj, A. Shaheen, J. Xu, P. Estrela, A. Mujahid, T. Asim, M. Zubair Iqbal, W.S. Khan, S.Z. Bajwa, In-situ synthesis of 3D ultra-small gold augmented graphene hybrid for highly sensitive electrochemical binding capability, J. Colloid Interface Sci. 553 (2019) 289–297.
[50] W. Huang, S. Wang, C. Guo, X. Yang, Y. Li, Y. Tu, Synthesis and characterization of well-defined poly(l-lactide) functionalized graphene oxide sheets with high grafting ratio prepared through click chemistry and supramolecular interactions, Polymer 55 (2014) 4619–4626.
[51] S.K. Sharma, M. Micic, S. Li, B. Hoar, S. Paudyal, E.M. Zahran, R.M. Leblanc, Conjugation of carbon dots with beta-galactosidase enzyme: surface chemistry and use in biosensing, Molecules (2019) 24.
[52] C. Luo, W. Wen, F. Lin, X. Zhang, H. Gu, S. Wang, Simplified aptamer-based colorimetric method using unmodified gold nanoparticles for the detection of carcinoma embryonic antigen, RSC Adv. 5 (2015) 10994–10999.
[53] N. Shahbazi, S. Hosseinkhani, B. Ranjbar, A facile and rapid aptasensor based on split peroxidase DNAzyme for visual detection of carcinoembryonic antigen in saliva, Sensor. Actuator. B Chem. 253 (2017) 794–803.
[54] H. Miao, L. Wang, Y. Zhuo, Z. Zhou, X. Yang, Label-free fluorimetric detection of CEA using carbon dots derived from tomato juice, Biosens. Bioelectron. 86 (2016) 83–89.
[55] B. Bao, P. Su, J. Zhu, J. Chen, Y. Xu, B. Gu, Y. Liu, L. Wang, Rapid aptasensor capable of simply detect tumor markers based on conjugated polyelectrolytes, Talanta 190 (2018) 204–209.
[56] Y. Wang, Z. Wei, X. Luo, Q. Wan, R. Qiu, S. Wang, An ultrasensitive homogeneous aptasensor for carcinoembryonic antigen based on upconversion fluorescence resonance energy transfer, Talanta 195 (2019) 33–39.
[57] W. Qin, K. Wang, K. Xiao, Y. Hou, W. Lu, H. Xu, Y. Wo, S. Feng, D. Cui, Carcinoembryonic antigen detection with "Handing"-controlled fluorescence spectroscopy using a color matrix for point-of-care applications, Biosens. Bioelectron. 90 (2017) 508–515.
[58] H. Khang, K. Cho, S. Chong, J.H. Lee, All-in-one dual-aptasensor capable of rapidly quantifying carcinoembryonic antigen, Biosens. Bioelectron. 90 (2017) 46–52.
[59] Y.L. Wang, J.T. Cao, Y.H. Chen, Y.M. Liu, A label-free electrochemiluminescence aptasensor for carcinoembryonic antigen detection based on electrodeposited ZnS–CdS on MoS_2 decorated electrode, Analytical Methods 8 (2016) 5242–5247.
[60] H. Shu, W. Wen, H. Xiong, X. Zhang, S. Wang, Novel electrochemical aptamer biosensor based on gold nanoparticles signal amplification for the detection of carcinoembryonic antigen, Electrochem. Commun. 37 (2013) 15–19.
[61] J. Xiang, X. Pi, X. Chen, L. Xiang, M. Yang, H. Ren, X. Shen, N. Qi, C. Deng, Integrated signal probe based aptasensor for dual-analyte detection, Biosens. Bioelectron. 96 (2017) 268–274.